



Full Length Article

Forces of Flow and Plant Resistance: Elucidation using *Tamarix chinensis* as a Model Species

Hongyi Sun¹, Haitao Dong¹, Wenzhi Zhao², Jianjun Kang² and Le Liu³

¹Key Laboratory of Desert and Desertification, Northwest Institute of Eco-Environment and Resources, Chinese Academy of Science, Lanzhou 730000, Gansu, China

²Linze Inland River Basin Research Station, Northwest Institute of Eco-Environment and Resources, Chinese Academy of Science, Lanzhou 730000, Gansu, China

³University of Chinese Academy of Sciences, Beijing 100049, Beijing, China

*For correspondence: sunhy569@lzb.ac.cn

Abstract

In this research, an attempt was made to reveal the forces of flow and plant resistance using *Tamarix chinensis* as a representative species. Results indicated that rigidity and flexibility coexist within the same plant, with an inflection point between the two properties. Branch length from the base to the inflection point exhibited the rigid zone, with logarithmic growth as the diameter class increased and low variability in length. The flexible zone was located between the inflection point and top of the stem and its length was stable in this range. A size range of stem-diameters contributed a series of inflection points, the resistance of the series and the height of the rigid zone exhibited exponential growth as the diameter class increased. A series of inflection points can produce an inflection points in the 15–20 mm diameter class. This indicates that beyond the inflection point, the resistance increases noticeably with the increase in diameter class. These findings suggest that the rigidity and flexibility of *T. chinensis* is a relative concept, and thus an absolutely rigid or flexible plant may not exist. © 2018 Friends Science Publishers

Keywords: Rigidity; Flexibility; Resistance; *Tamarix chinensis*; Inflection point

Introduction

Rigidity and flexibility in plants are rarely studied in environments with wind-driven sand flow deserts. In deserts, plant's rigidity offers resistance to sand, while flexibility offers plant survival and both properties are critical to desertification control. *Tamarix chinensis* Lour. (Family: Tamaricaceae) is a typical perennial xerophyte having strong resistance against damages caused by sandstorms in deserts. The species has many properties similar to aquatic plants and is a preferred material to study the rigidity and flexibility of plants under desert conditions. Plants growing in moving water have the same fluid force-bearing characteristics as those inhabiting windy or sandy environments (Tang, 2008; Zhang and Yang, 2010). Rigid parts of plants growing in aquatic habitats change vertical distribution and reduce velocity of water flow and often raise water level. In rivers, this could help to increase resistance to water-flow thereby reducing the flood-discharge capacity of rivers (Yen, 2002). Flexible parts of plants cause sediment deposition in rivers, exerting positive effects on river habitats, bank protection and water purification (Li and Shen, 1973; Jordanova and James, 2003; Yan *et al.*, 2004). Investigations of the resistance,

avoidance and tolerance strategies of plants to mechanical forces have shown that they are negatively correlated across species.

Plants growing in sandy environments also have rigidity and flexibility characteristics to help them change ground roughness and wind-flow near the ground. This allows plant parts above the ground to create an effective sand-stabilization condition (Shi and Cao, 2000; Tang *et al.*, 2011). The widely-used traditional Chinese sand-stabilization technology makes a full use of the rigidity and flexibility of straw to achieve effective sand-fixation with straw-checkerboard barriers (Shapotou Desert Research Station of Lanzhou Desert Institute, 1991 Personnel Communication). Plant biomechanical properties such as rigidity and flexibility are characterized by high variability with regard to environment, species and scales (Paul *et al.*, 2012; Albayrak *et al.*, 2014; Miler *et al.*, 2014) and represent a challenge for development of analytical and numerical models for deformation of simple-shaped flexible elements (Chen *et al.*, 2011; Kubrak *et al.*, 2012; Stone *et al.*, 2013; Boothroyd *et al.*, 2017).

T. chinensis is a perennial shrub that develops and survives in river channels in desert areas and also grows well in saline-alkali soils (Shafroth *et al.*, 1995;

Matthew, 2009). It mainly comes from the temperate and subtropical deserts arid and semi-arid deserts and steppe areas (Zhang *et al.*, 2003a, b). During the growing seasons from April to September, *T. chinensis* produces extremely small seeds which can disperse by wind or water and rapidly germinate in wet areas (Everitt, 1980; Roelle and Gladwin, 1999). After one year of growth, *T. chinensis* roots can produce several clonal ramets which will develop into new plants after alluvial sand deposition (Everitt, 1980). *T. chinensis* is a facultative phreatophyte which can endure long periods of drought stress because its main root is highly developed and can extend to deep groundwater (Cleverly *et al.*, 1997; Shafroth *et al.*, 2000). Vertical growth is the primary, and ground-sticking and eccentric growth, adventitious budding and branch agglutination are secondary characteristics which demonstrate maturity in *T. chinensis* (Sun *et al.*, 2014). Therefore, *T. chinensis* may be a model material for the study of rigidity and flexibility in desert plants.

In this study, quantification of the relationships between rigidity and flexibility was studied in *T. chinensis*. The branch rigidity and flexibility of fasciculate *T. chinensis* of six different age classes having stem diameter: 0–5, 5–10, 10–15, 15–20, 20–25 and 25–30 mm were studied.

Materials and Methods

Study Site

The present study was conducted on the bank of the Dasha River (39°17' 7" N, 100°11' 27" E) near the oasis in Linze County, Gansu Province, northwestern China. The Dasha River flows seasonally from south to north and the riverbed consists of coarse sands (Fig. 1). The average annual precipitation and evaporation in the area are 116.8 mm and 2390 mm, respectively. The mean annual temperature is 7.6°C, with the highest temperature in July (39.1) and the lowest in January (-27.0°C). The mean annual duration of sunshine is 3045 h and the mean annual accumulated temperature above 10°C is 3088°C. The frost-free period in the region is 165 d. The prevailing winds are from the Northwest, with a windy period from March to May. The average annual wind speed and the average days of gale are above class 8 and 3.2 m.s⁻¹, respectively. In the study site, the base diameter (determination of vernier caliper) of 8 and 1 year old *T. chinensis* saplings were recorded as 27.45 and 4.73 mm, respectively.

Experimental Design

Samples were collected from wild-growing plants at Yanuan Village on the Dasha River bank on March 26, 2014. Forty-two branches from a cluster of *T. chinensis* were wholly cut off from the roots and taken to the laboratory. Considering the base diameters, they were separated into 6 classes (Table 1). These are 0–5, 5–10, 10–

15, 15–20, 20–25 and 25–30 mm. In the diameter classes as mentioned before the number of branches taken were 6, 10, 6, 10, 6, and 4, respectively. The experimental samples of branch bases were prepared after Stone *et al.* (2014). By using a spring tension meter, normal force was applied in brief to every branch (Fig. 2). The resistance positions deviated 15°, 30°, 45°, 60° and 75°, respectively from the vertical direction (Fig. 3). To avoid deformation of branches, force was applied every 10 cm interval to branches of small diameter classes and every 20 cm intervals to those of large diameter branches. Resistance measurements started from points of flexibility and progressed to points of rigidity. The measurement was carried out when the diameter of each branch was shrunk by 1 mm until the resistance could not be measured at all (Fig. 3). Different branch-resistance measurements were conducted with corresponding spring tension meters, so that resistance forces of small branches were measured by small-range or high-precision tension meters, while those of large branches were measured by large-range or applicable-precision tension meters (Table 2).

Determination of Rigid Flexible Zones and of Inflection Points

According to Liu *et al.* (2008), when a single branch is pulled into a curve under the action of an external force, the convex and concave boundary point of the curve are defined as an "inflection point" (Fig. 4). The distance between the ground and the inflection point is the rigid zone, while the distance between the inflection point and the top of the branch is the flexible zone (please see light-blue box, Fig. 4). The inflection points of consecutive diameter sizes from small to large constitute a series of inflection points (please see series of circles, Fig. 4). The value of a series of inflection points significantly increased for certain diameter classes and was defined as the "inflection point of inflection points" (red lightning in Fig. 4).

Determination of Z0 Value

In the present study, no correlation was found between basal diameter and height of the adult population of *T. chinensis* indicating that the rigidity zone had fixed values (Sun *et al.*, 2014). The fixed values had a stronger resistance to water flow or wind-sand flow than the flexible zone. Therefore, in the present study the range of plant height has been defined as Z0.

Results

Growth Features of *T. chinensis* Saplings

Base diameter and height (Fig. 5A, R²=0.559) and base diameter and annual ring (Fig. 5B, R²=0.535) were positively correlated for 42 fasciculate branches of a cluster of *T. chinensis* growing in the floodplain.

Table 1: Base diameter classes of *T. chinensis*

Groups	1	2	3	4	5	6
Base diameter classes (mm)	0-5	5-10	10-15	15-20	20-25	25-30
Replicates	6	10	6	10	6	4

Table 2: Type and precision of instruments

Type	Limit load	recision
LTZ-50	500N	0N
LTZ-10	100N	N
LTZ-5	50N	N
LTZ-1	10N	.2N

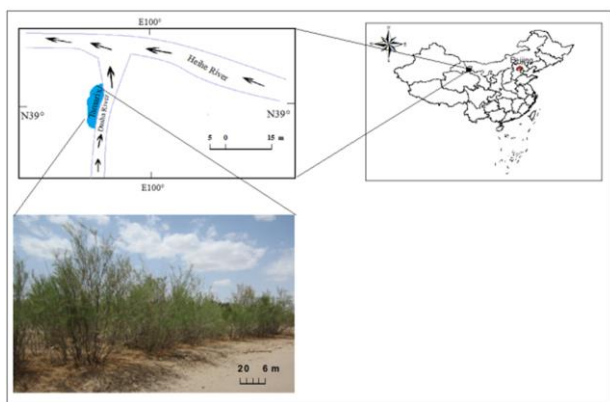


Fig. 1: Distribution of *T. chinensis* on the bank of Dasha River in Yanuan Village, Linze County, Gansu Province, Northwest China

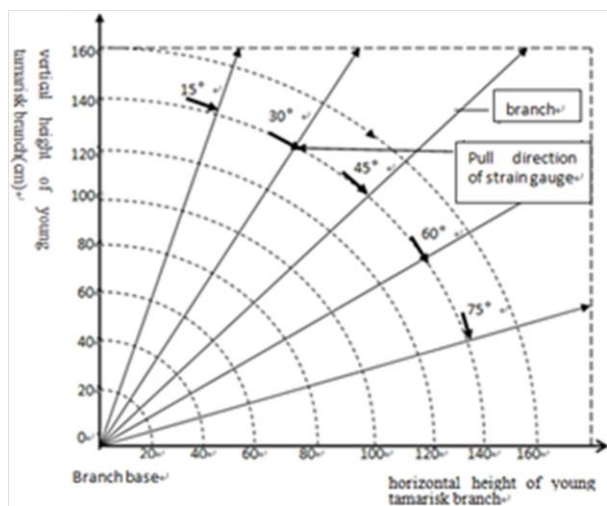


Fig. 2: Test model of *T. chinensis* resistance measurement

Resistance Distribution of *T. chinensis* Branches at Different Heights

Resistance relationships at different positions and heights: When resistance positions of *T. chinensis* branches at different heights deviated 15°, 30°, 45°, 60° and 75°,



Fig. 3: Mapping of normal forces given by tension meters (resistance forces to plants)

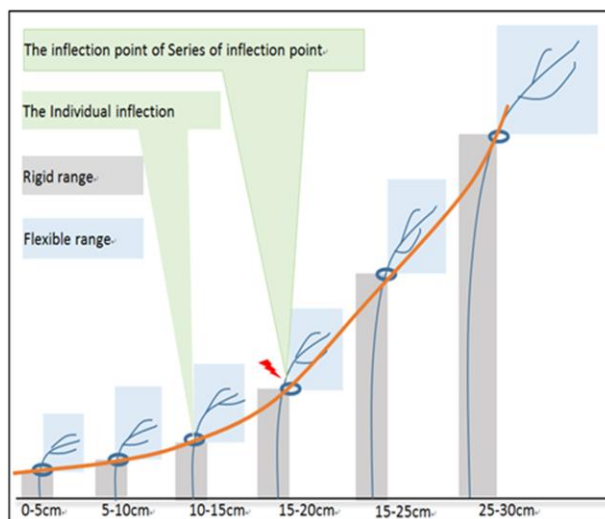


Fig. 4: A sketch of a series of inflection points for a range of diameters (shown as circles), and the inflection point of the series (shown as red lightning)

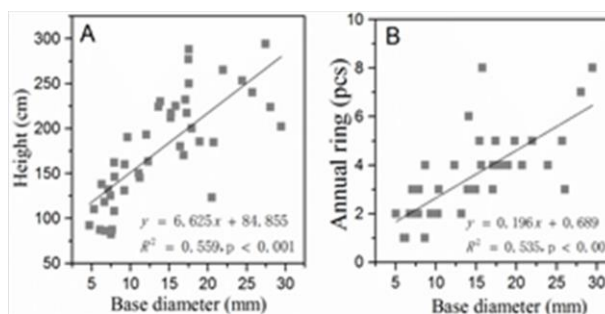


Fig. 5: Regression analyses between base diameter and height (A) and annual ring (B) of *T. chinensis* saplings (n=42)

respectively from the vertical direction (Fig. 6), the order of corresponding resistance forces was 75°>60°>45°>30°>15°. This indicated that the farther the branch deviated from its vertical position, the larger the resistance force exerted by the plant as branch height increased (Fig. 6A, C, E, G, I and K).

Table 3: The inflection point parameters for branches of different base diameters

Base diameter (mm)	Resistance force at inflection point (N)	Diameter at inflection Point (mm)	Flexible resistance range (N)	Rigid resistance range (N)	Rigid branch height (cm)	Flexible branch height (cm)													
0-5	1	4.4	0-1	1-17	0-25	25-50													
5-10	2.5	6	0-2.5	2.5-25	0-60	60-180													
10-15	5	8	0-5	5-55	0-80	80-190													
15-20	10	0-10	10-90	0-90	90-250	20-25	25	18	0-25	25-130	0-100	100-240	25-30	50	22	0-50	50-230	0-120	120-220
20-25	25	18	0-25	25-130	0-100	100-240													
25-30	50	22	0-50	50-230	0-120	120-220													

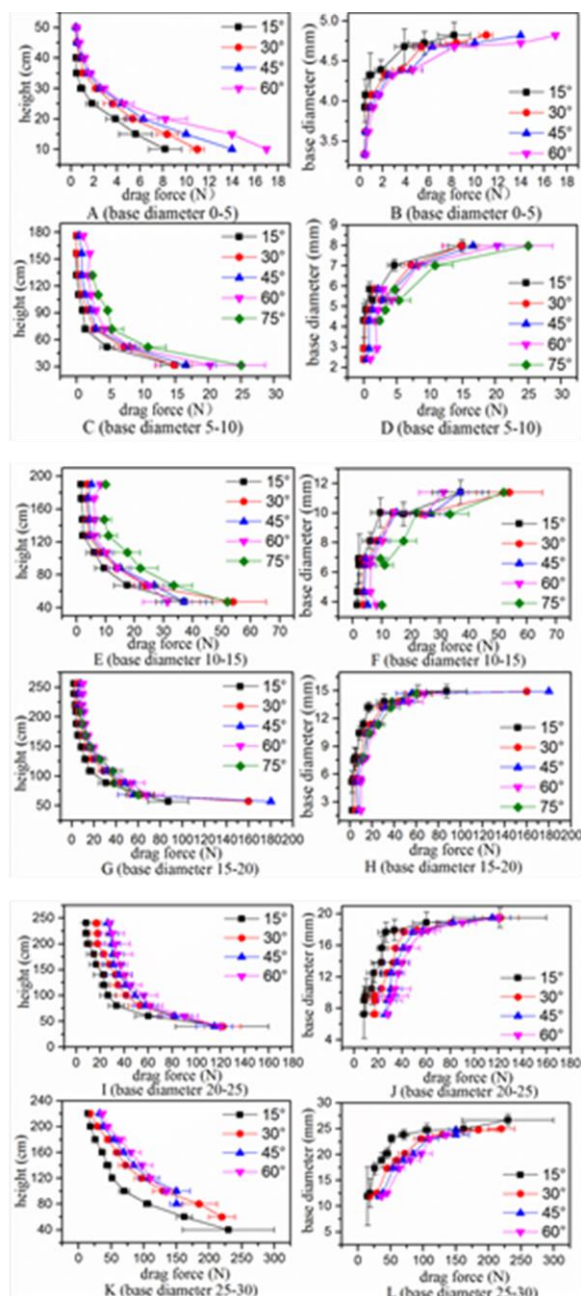


Fig. 6: Height of the rigid and flexible zones of branches for 6 diameter classes (0–5, 5–10, 10–15, 15–20, 20–25 and 25–30 mm), and corresponding resistance forces

Resistance changes of *T. chinensis* branches of having different diameters: The farther the branch deviated from its former position, the larger the resistance force exerted by the plant as the diameter class decreased (Table 3 and Fig. 6B, D, F, H, J and L). The rigid zone commenced from the largest base diameter, branch heights from 0–25 cm and resistance forces from 17 to 1 N (Fig. 6A), while the flexible zone with branch heights ranging from 25–50 cm exhibited resistance forces from 1–0 N. Therefore, the taller the branch, the more flexible, and the smaller the resistance force that it offered. When the flexibility reached the maximum, resistance no longer operated (Fig. 6A). Accordingly, branches with heights ranging from 0–25 cm were rigid, those with heights ranging from 25–50 cm were flexible and the inflection point that altered *T. chinensis* from rigidity to flexibility was found when the resistance force was 1 N. Plant resistance exhibited large variability in the range of rigidity (17-1 N) and uniformity in the range of flexibility (1–0 N) (Fig. 6B). The inflection point (change from rigidity to flexibility) was found at the height of 25 cm with a corresponding diameter of 4.4 mm (Fig. 6B). Thus branches with diameter classes 0–5 mm, base diameters of 4.4–5.0 mm, and heights of 0–25 cm rated in the range of rigidity, while those with base diameters of 0–4.4 mm and heights of 25–50 cm rated in the range of flexibility. Flexible resistance data were not obtained when diameter was 3.3 mm. This indicated that the larger the diameter, the higher the force of resistance, and the smaller the diameter, the lower the force of resistance. Also, the smaller the diameter, the closer to flexibility the branches approach, with flexibility reaching maximum at the top of the branches.

Branches with a diameter class of 0–5 mm exhibited both rigidity and flexibility. The minimum resistance force in the range of rigidity (17–1 N) was the maximum resistance force in flexibility, which was also at the inflection point shifting rigidity to flexibility. In the flexible range with resistance forces 1–0 N, the flexible resistance force was 0 at the top of the branch. At the inflection point, branch diameter was 4.4 mm, resistance force was 1 N and the rigid branch height was 25 cm. Beyond the inflection point, the length of flexible branches ranged from 25–50 cm.

Inflection points, resistance forces, diameters at inflection points, rigid resistance ranges and heights and flexible resistance ranges and heights can be obtained when

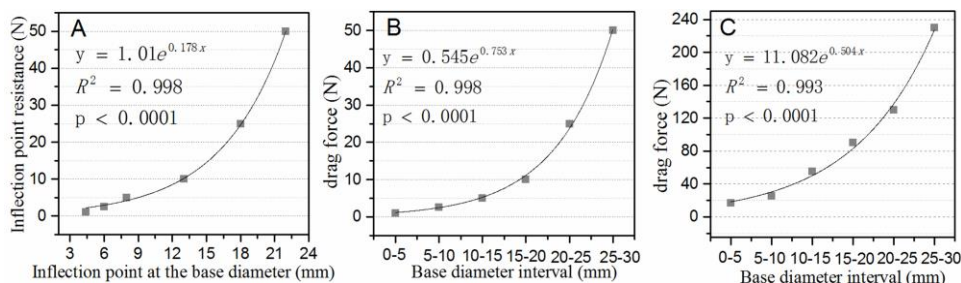


Fig. 7: Inflection point resistance features of *T. chinensis* branches for different diameter classes

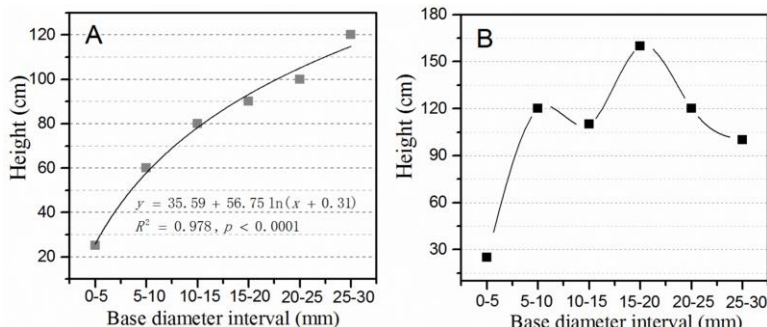


Fig. 8: Rigid and flexible branch heights of *T. chinensis* saplings with different base diameters

diameter classes are 5–10 mm (Fig. 6C and D), 10–15 mm (Fig. 6E and F), 15–20 mm (Fig. 6G and H), 20–25 mm (Fig. 6I and J) and 25–30 mm (Fig. 6K and L), respectively (Table 3).

Discussion

T. chinensis germinates and grows well in the floodplain. When the riverbed dries up and stone or sand is exposed, the seedlings exhibit erect growth, similar to branches developing on adult plants. Lower parts of *T. chinensis* branches are rigid, while the upper parts are flexible and the points of transition from rigidity to flexibility are inflection points. It is found that rigidity and flexibility coexist in *T. chinensis* and are critical in rivers and in windy or sandy environments, for they combine to result in resistance to fluids. The results of the present study differ from those of previous ones, in respect to that rigid plants cannot be simplified to matters concerning steady flow through rigid tubes in river-flume tests (Huang *et al.*, 1999; Bouma *et al.*, 2005; Hamimed *et al.*, 2013; Silinski *et al.*, 2015) or wind tunnel tests in windy or sandy environments (Wasson and Hyde, 1983; Musick and Trujillo, 1996; Ma *et al.*, 2006; Wu *et al.*, 2006; Li *et al.*, 2007a, b). In previous studies, the general characteristics of the longitudinal velocity profiles within the dowel array for both emergent and submerged flows at locations in line with the dowels are a velocity spike near the bed. This is followed by an inflection point that leads to a region of lower constant velocity throughout most of the flow depth. The velocity then

increases slightly near the free surface. Under submerged conditions, the increase in velocity is accompanied by an inflection point just below the top of the dowel array.

The inflection points are associated with coherent structures formed by the mixing of different velocity fluids that are dominated by counterclockwise vortices in the vicinity of the bed and clockwise vortices at the top of the dowels. Under high-density dowel configurations, the velocity measurements above the dowel array collapse onto a single logarithmic profile. The bulk velocity within the canopy portion of the flow, for experiments having the same dowel configuration, is very similar despite having large differences in flow rates for emergent and submerged dowels. Therefore, its value is marginally dependent on the overall flow rate. The inflection point in the present study is different from that described by (Liu *et al.*, 2008). When plant flexibility is replaced by a horsehair-type soft material (Wu *et al.*, 1999), the behavior of submerged plants and their crowns is not fully represented, because flexible and rigid obstacles to flow are not taken into account. When branches of plants were used, with two ends dragged in opposite directions, the ultimate strength that broke the branches was thought of as the plant resistance to air flow (Ge *et al.*, 2013). However, this cannot be taken as the resistance of plant to air flow. On the contrary, with the help of descriptions of wall resistance (James *et al.*, 2004), traverse resistance is used to indicate the plant resistance to air flow, which reasonably explains rigidity and flexibility of plants. Järvelä (2004), aiming to determine flow

resistance by comparing leafless with leafy plants, concluded that only herbaceous plants cannot explain the role of an inflection point.

Within the rigid parts of small to large branches, we found that in correlations of branch diameters and resistance forces at inflection points (Fig. 7A: $y = 3.4549x$, $R^2 = 0.959$), diameter classes and resistance forces at inflection points (Fig. 7B: $y = 0.4853e0.776x$, $R^2 = 0.998$), and base diameters and resistance forces at base diameters (Fig. 7C: $y = 9.8276e0.4912x$, $R^2 = 0.9828$), the resistance forces increased as an exponential function with the increase in base diameters. Diameter class 15–20 mm was at the parting line; rigid resistance forces were small (10–90 N) when base diameters were small (0–5, 5–10 and 10–15 mm), and rigid resistance forces were large (50–230 N) when base diameters were large (20–25 and 25–30 mm). Therefore, diameter class 15–20 mm was at the inflection point for rigidity between small to large diameter classes. Based on these trends (Fig. 7A, B and C), resistance forces at inflection points will increase. As can be predicted, resistance forces at inflection points will continue to increase with the increase in branch diameters in *T. chinensis*, but this relationship needs to be confirmed for other species.

Sand-fixing plants have been classified according to their flexibility as follows: most shrubs and semi-shrubs are generally rigid because they have a high degree of lignification and their stems are thick and hard. But herbs, especially plants belong to Poaceae, are flexible because they have a low degree of lignifications and exhibit noticeable elasticity and pliability. *Salix mongolica* and *T. chinensis*, as shrubs with lignified branches, also belong to the flexible-plant group because they exhibit a high degree of pliability (Tang *et al.*, 2011). In this study, it is seen that such a qualitative system did not reflect the dynamics of rigidity and flexibility in plants, because rigidity and flexibility differed with diameter classes in *T. chinensis* and possibly in other plants. Additionally, fewer psammophyte than aquatic plant species are flexible plants and they are only lightly affected by population density because of water deficit and sparse distribution of individuals in arid and semi-arid areas. We conclude that the definition of flexibility in psammophyte species is relatively easier than in other species and we differ in that from previous work (Qu *et al.*, 2012). Thus, finding other indicators of flexibility in this study was not necessary to establish this definition. Interestingly, studies on the effects of water flow on seagrass bending showed that an underlying current exerts the initial force which causes the plants to bend. This bending leads to a primary tension within the blades and the force required bending the blade further increases with an increase in the angle of bending (Paul *et al.*, 2012). Our results with small-diameter branches support this view and the canopy mixing-layer model applied to highly-flexible aquatic vegetation (Marjoribank *et al.*, 2017).

The zone of rigidity in *T. chinensis* branches extended from branch base to the inflection point (Table 3 and Fig. 8A). With an increase in diameter classes, the length of the branch rigid zone showed logarithmic growth ($y = 49.803\ln(x) + 24.555$, $R^2 = 0.9864$). Though there still exists growth room above the diameter class 25–30 cm, the trend was stable. We concluded that the length and base diameter of adult *T. chinensis* population was not correlated, which also explained why rigidity in *T. chinensis* was a fixed value (Sun *et al.*, 2014; Aberle and Järvelä, 2015). This fixed value was the surface roughness ZO of water or wind-sand flow. Our results supported the expectation that no trees would bend to a height lower than approximately 42% of their original height, even in water moving at 2.5 m/s (Stone *et al.*, 2013). Thomas (1975) found in psammophyte plants growing in temperate coastal dunes that ZO of rigid 50 cm high plants is 9.0 cm, while ZO of flexible plants of the same height is 5.0 cm. Flexibility of *Salix* sp., *Populus simonii* sp., *Artemisia ordosica*, and some common psammophyte plants on the Mu Us Sandland changed along with the increase in plant stem cross-sectional area, where *A. ordosica* showed the greatest variation, and *Salix* reached the minimum (Tang, 2008). *Salix* stem flexibility was stable with changes in cross-sectional area, while *A. ordosica* flexibility was lower when its stem was wider (Qu *et al.*, 2012). Our study supports such qualitative results by quantifying the resistance forces.

The length of flexible parts of different diameter *T. chinensis* extended from the inflection point to the tip of branches (Table 3 and Fig. 8B). Starting at diameter class 5–10 mm, flexible length was basically fixed in the range of 100–160 cm (Table 3). The variability in the flexible branch length was also fixed. Flexible branches grow mainly plant leaves, provide shade for the ground, and support photosynthesis. They have less impact on fluid movement than rigid branches do, but they can change the spatial structure of fluids, and lessen the impact of wind speed on sand-fixing ability of plant (Tang *et al.*, 2007; 2011). Our study supports the earlier results by quantifying the resistance forces.

Conclusion

Rigidity and flexibility of *T. chinensis* is a concept relative to a specific plant and plants exhibiting absolute rigidity or flexibility may not exist. Studies on rigidity and flexibility of plants are important for the management of river flow and control of desertification. Shrubs and arbors are typical desert species with strong resistance to the abrasive forces of wind-sand flow, and dual characteristics of rigidity and flexibility. Our results increase the understanding of the role of plant size and growth stage in control of desertification, clarify the function of plant resistance to changes in water-flow velocity and sediment deposition, and help reveal how plants support the process of changing desert soils into productive soils.

Acknowledgements

This work was supported by the Chinese National Natural Science Foundation (Grant No. Y511601001) and the Key Project of Chinese National Programs (973 Program) for Fundamental Research and Development (Grant No. 2013CB956000). We are very grateful to the anonymous reviewers as well as editors for their constructive comments, which improved the overall quality of the manuscript.

References

- Aberle, J. and J. Järvelä, 2015. *Hydrodynamics of Vegetated Channels. Rivers-Physical, Fluvial and Environmental Processes*, pp: 519–541. Springer International Publishing
- Albayrak, I., V. Nikora, O. Miler and M. O'Hare, 2014. Flow-plant interactions at leaf, stem and shoot scales: drag, turbulence, and biomechanics. *Aquat. Sci.*, 76: 269–294
- Boothroyd, R.J., J. Hardy, R.J. Warburton and T.I. Marjoribank, 2017. Modeling complex flow structures and drag around a submerged plant of varied posture. *Water Resour. Res.*, 53: 2877–2901
- Bouma, T.J., M.B. De Vries, E. Low, G. Peralta, I.C. Tanczos, J. van de Koppel and P.M.J. Herman, 2005. Trade-offs related to ecosystem engineering: a case study on stiffness of emerging macrophytes. *Ecology*, 86: 2187–2199
- Chen, L., M.C. Stone, K. Acharya and K.A. Steinhaus, 2011. Mechanical analysis for emergent vegetation in flowing fluids. *J. Hydraul. Res.*, 49: 766–774
- Cleverly, J.R., S.D. Smith, A. Sala and D.A. Devitt, 1997. Invasive capacity of *Tamarix ramosissima* in a Mojave Desert floodplain: The role of drought. *Oecologia*, 111: 12–18
- Everitt, B.L., 1980. Ecology of salt cedar—a plea for research. *Environ. Geol.*, 3: 77–84
- Ge, R.L., Q. Si and J.Y. Liu, 2013. Branches tensile mechanical characteristics and the influencing factors of six plant species in inner Mongolia. *J. Des. Res.*, 33: 1333–1339
- Hamimed, A., L.M. Nehal, M. Benslimane and A. Khaldi, 2013. Contribution to the study of the flow resistance in a flume with artificial emergent vegetation. *Lar. J.*, 15: 55–63
- Huang, B.S., G.W. Lai, J. Qiu and P. Wan, 1999. Experimental research on influence of vegetated floodplains upon flood carrying capacity of River. *J. Hydrodyn.*, 14: 76–82
- James, C.S., A.L. Birkhead, A.A. Jordanova and J. JO'Sullivan, 2004. Flow resistance of emergent vegetation. *J. Hydraul. Res.*, 42: 390–398
- Jordanova, A.A. and C.S. James, 2003. Experimental study of bed load transport through emergent vegetation. *J. Hydraul. Eng.*, 129: 474–478
- Järvelä, J., 2004. Determination of flow resistance caused by non-submerged woody vegetation. *Int. J. River Basin Manage.*, 2: 61–70
- Kubrak, O.L., B.M. Rovenko, V.V. Husak, J.M. Storey and K.B. Storey, 2012. Nickel induces hyperglycemia and glycogenolysis and affects the antioxidant system in liver and white muscle of goldfish *Carassius auratus* L. *Ecotoxicol. Environ. Saf.*, 80: 231–237
- Li, R.M. and H.W. Shen, 1973. Effect of tall vegetations on flow and Sediment. *J. Hydraul. Div.*, 99: 793–814
- Li, Z.Z., S.L. Wu, C.X. Xiao, Q.M. Sun, L.M. Liu and Z.H. Zhang, 2007a. Study on wind-tunnel simulated flow pattern over Nabkha in Hetian river Basin, Xinjiang. *J. Des. Res.*, 27: 9–14
- Li, Z.Z., S.L. Wu, C.X. Xiao, L.M. Liu, Q.M. Sun and Z.H. Zhang, 2007b. Study on wind-tunnel simulated flow pattern over Nabkha in Hetian river Basin, Xinjiang. *J. Des. Res.*, 27: 15–19
- Liu, D., P. Diplas, J.D. Fairbanks and C.C. Hodges, 2008. An experimental study of flow through rigid vegetation. *J. Geophys. Res.*, 113: 66–83
- Ma, S.L., G.D. Ding, Y.G. Hao, H.J. Xiao and T.T. Yang, 2006. Experimental research of viscous flow around a *Nitraria tangutorum* boscage. *Res. Soil Water Conserv.*, 13: 146–149
- Marjoribank, T.I., R.J. Hardy, S.N. Lane and D.R. Parsons, 2017. Does the canopy mixing layer model apply to highly flexible aquatic vegetation? Insights from numerical modeling. *Environ. Fluid Mech.*, 17: 277–301
- Matthew, K.C., 2009. The monsterring of Tamarisk: How scientists made a plant into a problem. *J. History Biol.*, 42: 231–266
- Miler, O., I. Albayrak, V. Nikora and M. O'Hare, 2014. Biomechanical properties and morphological characteristics of lake and river plants: implications for adaptations to flow conditions. *Aquat. Sci.*, 76: 465–481
- Musick, H.B. and S.M. Trujillo, 1996. Wind-tunnel modeling of the influence of vegetation structure on saltation threshold. *Earth Surf. Process Landforms*, 21: 589–606
- Paul, M., T.J. Bouma and C.L. Amos, 2012. Wave attenuation by submerged vegetation: combining the effect of organism traits and tidal current. *Mar. Ecol. Prog.*, 444: 31–41
- Qu, Z.Q., L.Y. Liu, L.L. Yan, Y. Tang and Z.J. Jia, 2012. Application of concept of flexibility in psammophyte research. *J. Des. Res.*, 32: 42–46
- Roelle, J.E. and D.N. Gladwin, 1999. Establishment of woody riparian species from natural seed fall at a former gravel pit. *Restor. Ecol.*, 7: 183–192
- Shafroth, P.B., J.C. Stromberg and D.T. Patten, 2000. Woody riparian vegetation response to different alluvial water table regimes. *West N. Amer. Natur.*, 60: 66–76
- Shafroth, P.B., J.M. Friedman and L.S. Ischinger, 1995. Effects of salinity on establishment of populus fremontii, cottonwood) and *Tamarix ramosissima* (Salt cedar) in southwestern United States. *Great Basin Nat.*, 55: 58–65
- Shapotou Desert Research Station of Lanzhou Desert Institute, 1991. Shapotou section of Baolan railway period of sand-fixation principle and measures, Ningxia People's Publishing House: 95–105
- Shi, B. and S.Y. Cao, 2000. *Sand Plant Dynamics*, pp: 103–113. Qing Dao Ocean University Press, Qingdao, China
- Silinski, A., M. Heuner, J. Schoelynck, S. Puijalon, U. Schröder, E. Fuchs, P. Troch, T. Bouma, P. Meire and S. Temmerman, 2015. Effects of wind waves versus ship waves on tidal marsh plants: a flume study on different life stages of *Scirpus maritimus*. *PLoS One*, 10: e0118687
- Stone, M.C., L. Chen, S.K. McKay, J. Goreham, K. Acharya, C. Fischenich and A.B. Stone, 2013. Bending of submerged woody riparian vegetation as a function of hydraulic flow conditions. *River Res. Appl.*, 29: 195–205
- Stone, N.J., D.M. Lloyd-Jones, C. Blum, G.D. Jr and S.S. Jr., 2014. Letter by Stone et al regarding article, perspective on the 2013 American Heart Association/American college of cardiology guideline for the use of statins in primary prevention of low-risk individuals. *Circul. Res.*, 115: 1–2
- Sun, H.Y., W.Z. Zhao, Z.B. Dong and H.T. Dong, 2014. Statistical analysis of population characteristics of Tamarisk on the Yellow River Bank in Tongde, Qinghai. *Energy Education Science and Technology Part A: Ener. Sci. Res.*, 32: 8467–8478
- Tang, H.W., J. Yan and S.Q. Lu, 2007. Advances in research on flows with vegetation in river management. *Adv. Water Sci.*, 18: 785–792
- Tang, Y., 2008. Comparison on morphology and sand trapping capability of threeshrubs in south edge of Mu Us sandland. *Res. Soil Water Conserv.*, 15: 44–48
- Tang, Y., L.Y. Liu, Z.Q. Qu, H.U. Xia, L.L. Guo and L.L. Yan, 2011. Research review of capacity of plant for Trapping Blown Sand. *J. Des. Res.*, 31: 43–48
- Thomas, Y.F., 1975. *Actions Eoliennes en Milieu Littoral: Lapointe de la Courbe[M]*. Memoires delaboratoire degeomorphologie de l'ecoledeshautesetudes
- Wasson, R.J. and R. Hyde, 1983. Factors determining desert dune type. *Nature*, 304: 337–339

- Wu, F.C., H.W. Shen and Y.J. Chou, 1999. Variation of roughness coefficients for unsubmerged and submerged vegetation. *J. Hydraul. Eng.*, 125: 934–942
- Wu, S.L., Z.Z. Li, J. Hui, C.X. Xiao and Q.M. Sun, 2006. Study on the distribution character of surface pressure of Nabkha in Wind-tunnel Imitative Experiment. *Arid. Land Geog.*, 29: 790–796
- Yan, J., Z. Zhou and X.Y. Qiu, 2004. Transportation characteristics of bed load sediment of upper reaches end before vegetation dam. *J. Xinjiang Agric. Univ.*, 27: 67–72
- Yen, B.C., 2002. Open channel flow resistance. *J. Hydr. Eng.*, 128: 20–39
- Zhang, J.J. and P. Yang, 2010. Research progress of contain plant river problem. *Water Sci. Eng. Technol.*, 6: 32–35
- Zhang, D.Y., B.R. Pan and L.K. Yin, 2003a. The photogeographical studies of *Tamarix* (*Tamaricaceae*). *Acta. Bot. Yunnanica*, 25: 415–427
- Zhang, D.Y., L.K. Yin and B.R. Pan, 2003b. Study on drought-resisting mechanism of *Tamrix* L. and assessing of its potential application. *J. Des. Res.*, 23: 252–256

(Received 19 January 2018; Accepted 23 April 2018)